
STRUCTURE, PHASE TRANSFORMATIONS,
AND DIFFUSION

Molecular-Dynamic Simulation of the Bombardment of a Lead Film on Graphene by Xe₁₃ Clusters

A. E. Galashev

*Institute of High-Temperature Electrochemistry, Ural Branch, Russian Academy of Sciences,
ul. S. Kovalevskoi 22, Ekaterinburg, 620137 Russia
e-mail: alexander-galashev@yandex.ru*

Received December 16, 2014; in final form, September 22, 2015

Abstract—The purification of graphene from a lead film by irradiating the target with a beam of Xe₁₃ clusters with an energy of 20 eV at different angles of incidence has been studied. Using the method of statistical geometry, it has been shown that, before the bombardment, the double-layer lead film adsorbed on graphene had an irregular structure. Graphene contained divacancies, the edges of which, as well as the edges of the graphene sheet, were hydrogenated. The complete removal of lead from graphene was achieved at the angle of incidence of Xe₁₃ clusters equal to 45°. A major part of the film was separated from graphene in the form of an island, which, after separation, was transformed into a three-dimensional structure. The stresses present in the graphene sheet changed in the course of bombardment, but the stressed state retained after the bombardment was terminated. The type of the distribution of stresses in graphene indicates the absence of enhancement of the stressed state in the course of bombardment. The bombardment at angles of incidence of clusters less than 75° substantially enhances the roughness of graphene. The bombardments in the entire range of the angles of cluster incidence (0°–90°) have resulted in no significant damages in the hydrogenated edges of the graphene sheet.

Keywords: graphene, xenon clusters, stresses, film, lead

DOI: 10.1134/S0031918X16030054

INTRODUCTION

Lead is one of the most toxic metals. In natural biosphere, there are always trace amounts of various metals. The presence of some of them, even in a low concentration, requires fast oxidation because higher concentrations and products of lower degrees of oxidation can be dangerous. Unfortunately, the difference between the degrees of permissible and dangerous concentrations is usually small [1, 2]. One of the most abundant compounds that occur in nature in trace amounts is PbS. It is used as a cathode material in lithium batteries, in X-ray devices, as a pigment in domestic metallic mixtures, etc. The detection of industrial lead in the environment is a problem of great importance. Up to now, lead has been detected by such methods as spectrophotometry [3, 4], liquid–liquid extraction [5, 6], achievement of a cloud point [7, 8], and electrochemical measurements [9]. In recent years, the method of solid-state extraction is employed for analyzing traces of Pb. The trace amounts of Pb in aqueous media are determined using a surface-active substance covered by modified graphene-F-OH.

The removal of ultra-small amounts of heavy metals from air and water can be performed by applying filters with graphene membranes. However, in this case, the problem arises of purifying the filter from metallic sediment. Lead has a low adhesion energy with perfect graphene (0.2 eV) [10]; however, the binding energy of Pb atoms with graphene at the

boundary of a divacancy is quite appreciable (3.4 eV) [11]. It appears possible to remove a film of heavy metal by the bombardment with clusters of a noble gas [12–15]. The simulation of the process of the cluster bombardment has shown that to achieve a maximum effect, it is necessary that the entire energy transferred upon impact was released in a critical region near the surface [16–18]. It has been shown experimentally that upon the irradiation of the graphene surface by a beam of Xe atoms at the angle of incidence equal to 55°, the phonon modes of the surface receive approximately 20% less carried energy than in the case of a vertically directed beam [19]. In addition, Xe scatters from a smooth surface of graphite even if its energy makes up several tens of eV. To diminish the probability of damaging graphene upon the bombardment of the lead–graphene film, the graphene sheet was subjected to hydrogenation. The energies of the employed cluster beams are substantially less than the beam energies used in the experiments, the main task of which is the sputtering of substances.

The aim of this work is to conduct a detailed study of the process of a nondestructive removal of lead from the surface of partially hydrogenated imperfect graphene.

MOLECULAR-DYNAMIC MODEL

The interatomic interactions in graphene were represented by the many-body Tersoff potential [20]

modified so as to ensure a correct description of two-dimensional systems such as graphene. Since the original Tersoff potential does not have a barrier to the rotation about the single bond, the torsion potential [21] has been added to it, which allows one to eliminate the rotation of the graphene sheet. Note also that the simulation of graphene using the original Tersoff potential led to the cracking of the graphene sheet [22, 23]. Therefore, we increased the radius of covalent interaction from 0.21 to 0.23 nm and also included an additional weak attraction at $r > 0.23$ nm assigned by a Lennard-Jones (LD) potential with the parameters used in [21].

For simulation of atomistic interactions in the lead film, the many-body Sutton–Chen (SC) potential [24] was used. The SC potential energy is written as

$$U^{SC} = \varepsilon \left[\frac{1}{2} \sum_i \sum_{j \neq i} V(r_{ij}) - c \sum_i \sqrt{\rho_i} \right], \quad (1)$$

where

$$V(r_{ij}) = (a/r_{ij})^q, \quad \rho_i = \sum_{j \neq i} (a/r_{ij})^s. \quad (2)$$

Here, ε is a parameter with the dimensionality of energy; c is a nondimensional parameter; a is a parameter with the dimensionality of length, which is usually taken to be equal to the equilibrium lattice parameter; and q and s are positive integers with $q > s$.

The power-law form of the potential terms allows one to successfully combine the short-range interactions presented by the N -body term with a van der Waals tail that describes the long-range interactions.

The lead–carbon and xenon–xenon interactions were specified by a Lennard-Jones potential [25–27]. The interaction between Xe atoms and the atoms of the target (Pb and C) was assigned by the purely repulsive Ziegler–Biersack–Littmark (ZBL) potential [28]

$$\begin{aligned} \Phi = & Z_i Z_j \frac{e^2}{r} \left\{ 0.1818 \exp\left(-3.2 \frac{r}{a}\right) \right. \\ & + 0.5099 \exp\left(-0.9423 \frac{r}{a}\right) + 0.2802 \\ & \left. \times \exp\left(-0.4029 \frac{r}{a}\right) + 0.02817 \exp\left(-0.2016 \frac{r}{a}\right) \right\}, \quad (3) \end{aligned}$$

where Z_i and Z_j are the atomic numbers of the atoms i and j , e is the elementary electric charge, r is the interatomic distance, and the parameter a is determined by the expression

$$a = 0.8854 a_0 \left(Z_i^{0.23} + Z_j^{0.23} \right)^{-1}. \quad (4)$$

Here, a_0 is the Bohr radius. The shape of the ZBL potential is fitted by changing the coefficients at the exponents and at the powers of the exponents. Therefore, at equal values of r , the character of interaction of the components is defined by their atomic numbers. We neglect the weak attraction between the atoms of Xe and Pb and also between Xe and C, since the main

purpose of the present investigation is the examination of the transfer of energy and momentum, rather than of chemical bonding [29].

Defects that are present in graphene substantially increase the adhesion of metals at graphene. The most common defects in graphene are divacancies. The graphene sheet used for the lead deposition had four divacancies almost uniformly distributed over its surface. Hydrogenation was employed to strengthen the graphene edges and divacancy boundaries. The CH groups that were formed at the edges and at the sites closest to a divacancy center were simulated according to the monatomic scheme [30]. The C–CH and CH–CH interactions were represented via an LD potential [30]. The partial functionalization of graphene (via the connection of H atoms to its edges) stabilizes the structure without changing the interatomic spacings or creating roughness over the entire surface.

A film of lead on graphene was formed according to the procedure described in [13]. The numerical calculation of the equations of motion was performed by the Runge–Kutta method of the fourth order with a time step $\Delta t = 0.2$ fs. The bombardment at the angles of incidence equal to 0° , 45° , 60° , 75° , and 90° was performed with the kinetic energy of clusters equal to 20 eV by the method used in [13].

The impacts of clusters on the surface were accompanied by heating of the system. A moderate removal of the released heat from the system was performed using the Berendsen thermostat algorithm [31].

The density profile of the metallic film was calculated as follows:

$$\rho(z) = \frac{n(z) \sigma_{Pb}^3}{\Delta h S_{xy} N_s}, \quad (5)$$

where $n(z)$ is the number of Pb atoms in the layer parallel to the plane of the graphene; σ_{Pb} is the effective diameter of the Pb atom; Δh is the width of the layer; S_{xy} is the area of the graphene surface; and N_s is the number of tests.

The stress at the site of an atom i of the metallic film is defined as [24]

$$\begin{aligned} \sigma_{\alpha\beta}(i) = & \frac{\varepsilon}{2a^2 \Omega_i} \sum_{i \neq j}^k \left[-q (a/r_{ij})^{q+2} \right. \\ & \left. + cs (1/\sqrt{\rho_i} + 1/\sqrt{\rho_j}) (a/r_{ij})^{s+2} \right] r_{ij}^{\alpha} r_{ij}^{\beta}, \quad (6) \end{aligned}$$

where the volume Ω_i corresponding to an individual atom can be associated with the volume of the Voronoi polyhedron corresponding to atom i .

To calculate stresses that appear in graphene, the graphene sheet was divided into surface elements. The stresses $\sigma_{u\alpha}(l)$ that appear under the action of the forces of direction α ($\alpha = x, y, z$) are calculated on each element with the order number l , which has the orientation u . In these calculations, the products of

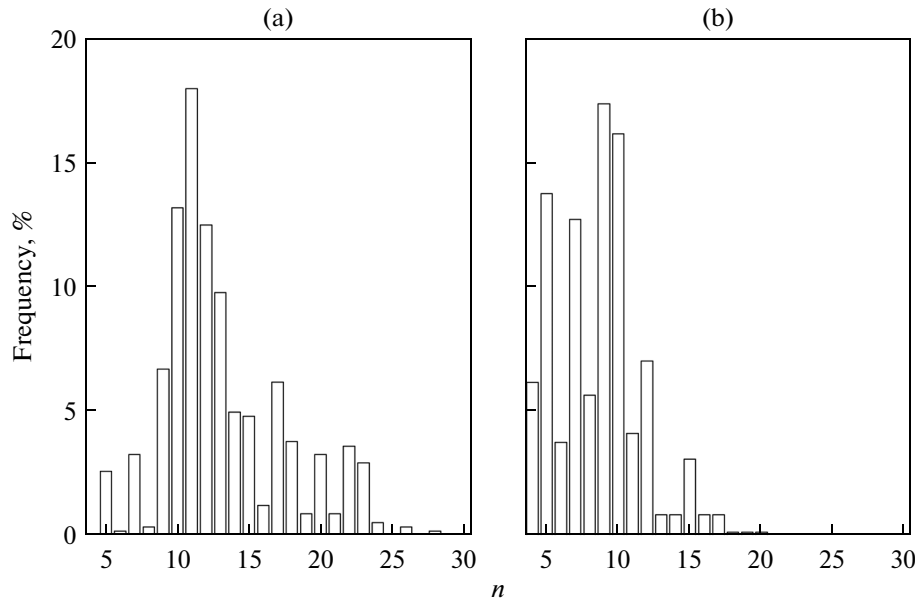


Fig. 1. Face-number distributions of (a) Voronoi polyhedra (VPa) and (b) simplified VPa for a lead film nonirradiated by a cluster beam on a modified graphene.

the projections of the velocities of atoms and of the projections of the forces f_{ij}^α acting on the l th element from the other atoms with the fulfillment of corresponding conditions [32] are used as follows:

$$\sigma_{u\alpha}(l) = \left\langle \sum_i^k \frac{1}{\Omega} (m v_u^i v_\alpha^i) \right\rangle + \frac{1}{S_l} \left\langle \sum_i^k \sum_{\substack{u_i \leq u, u_j \geq u \\ j \neq i}} (f_{ij}^\alpha) \right\rangle. \quad (7)$$

Here, k is the number of atoms on the element l , Ω is the volume per atom, m is the mass of an atom, v_α^i is the α projection of the velocity of atom i , and S_l is the area of the element l . The conditions for summation over j in the last sum in expression (7) are given in the lower and upper indices of the sum, the force that appears upon the interaction of atoms i and j goes through the l th element, and u_i is the current coordinate of the atom i . The upper index u in the last sum assigns the coordinate of the point at which the line connecting the centers of atoms i and j intersects the l th element.

The graphene sheet had dimensions of 3.4×2.8 nm and contained 406 C atoms. Each element l separated on this sheet and elongated along the axis oy (perpendicular to the zigzag direction of graphene) contained 14 C atoms and had an area of 0.68 nm². Specifically, this layout corresponds to the data shown in Fig. 6.

The roughness of the surface (or the arithmetic mean deviation of the profile) was calculated as

$$R_a = \frac{1}{N} \sum_{i=1}^N |z_i - \bar{z}|, \quad (8)$$

where N is the number of sites (atoms) on the surface of graphene, z_i is the level (height) of atom i , \bar{z} is the

level of the graphene surface, and the values z_i and \bar{z} are determined at the same time moment.

The total energy of a free one-sheet graphene obtained at $T = 300$ K is equal to -7.02 eV, which is in agreement with the quantum-mechanical calculation (-6.98 eV) [33]. The melting temperature T_m of a cluster Pb₂₀₁ with a free surface determined in a separate calculation is 417 K, which is in agreement with the MD calculations ($T_m = 412$ K) [34] also performed using the Sutton–Chen potential. In both cases, T_m has been determined based on the jump in the potential energy.

CALCULATION RESULTS

The deposition of Pb atoms on graphene performed in 1 million time steps resulted in a metal film with a very dense structure, which covered the entire graphene surface completely and almost uniformly. For a detailed analysis of the structure of this film, the method of statistical geometry was employed. Voronoi polyhedra (VPa) have been constructed for 30 atoms of Pb situated in the film in contact with graphene. The construction of these VPa is possible when in the least-populated half-space there is at least one atom. The VPa were defined by atom coordinates written in every 10000 time steps. In total, 3000 polyhedra were constructed. The most probable number (n_{mp}) of the nearest neighbors (including C atoms) in the film is equal to 11 (Fig. 1a), and the average number is $\bar{n} = 12.55$. The distribution of the simplified VPa obtained after the exclusion of edges with the length $l \leq 0.5\bar{l}$ (\bar{l} is the average length) has a maximum at $n_{mp} = 9$, whereas $\bar{n} = 8.14$ (Fig. 1b).

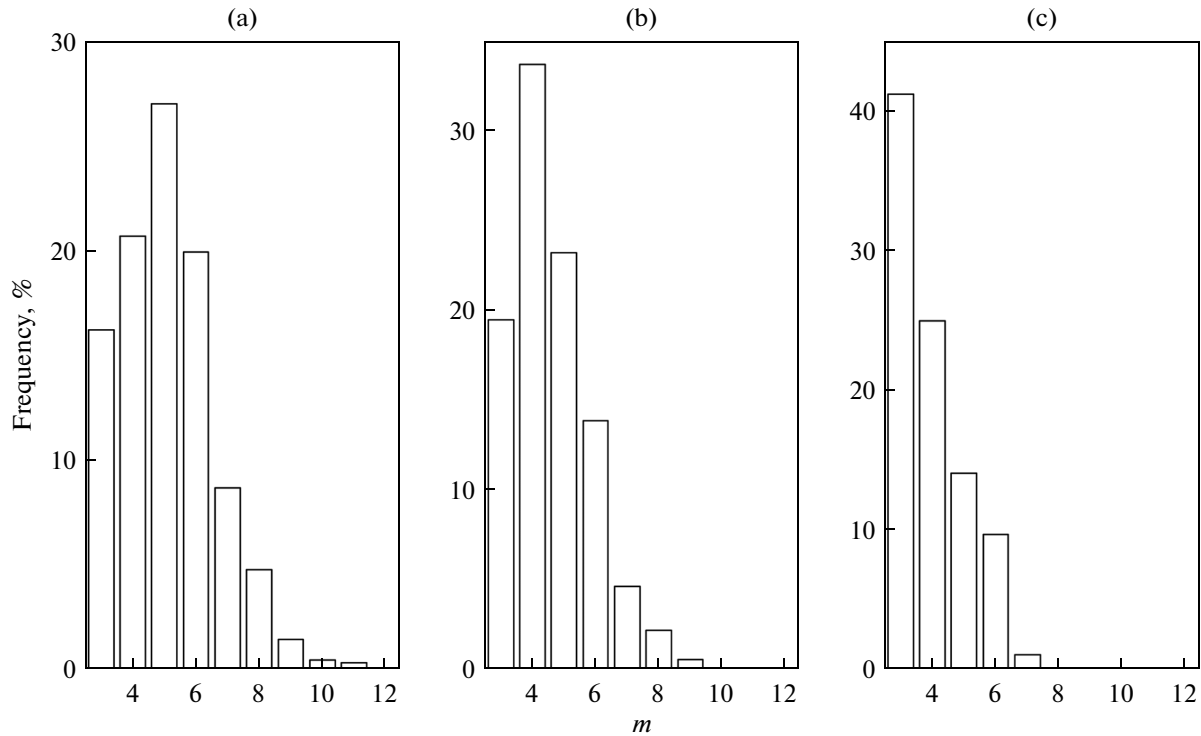


Fig. 2. Edge-number distribution of the faces of polyhedra for a lead film on modified graphene not subjected to the bombardment: (a) faces of VPa; (b) faces of simplified VPa; and (c) excluded small faces.

The most probable number of edges in a face (m_{mp}) in the case of VPa constructed for the Pb film is equal to 5 (Fig. 2a). The average number of edges in a face of the VPa is $\bar{m} = 5.09$. The obtained numbers m_{mp} and \bar{m} reflect a rotational symmetry of order 5. Therefore, the initial deposited Pb film had an irregular structure. In the case of simplified VPa, $m_{mp} = 4$ and $\bar{m} = 4.58$ (Fig. 2b). The analysis of the excluded small faces demonstrates that more than 40% of the faces are triangles, 25% are tetragons, and approximately 9% are pentagons (Fig. 2c). In the course of the bombardment with clusters of a heavy inert gas, especially at an angle of incidence $\theta = 0^\circ$, the film is densified and acquires a regular imperfect structure.

The result of 125 impacts by Xe_{13} clusters can be seen in Fig. 3, where the target configuration after the bombardment at the angles of incidence equal to 45° and 75° are shown. At an angle of 45° , the Pb film has separated completely from the graphene and acquired the shape of a cone, on top of which several atoms of Pb are adsorbed. The graphene sheet fringed by hydrogen atoms remained almost undamaged even in the region of divacancies. Quite a different picture is observed at the incidence angle of 75° . In this case, the Pb film is only partially removed from graphene; the majority of lead atoms remain connected to the graphene substrate. Just as in the case of the angle $\theta = 45^\circ$, the graphene preserves its integrity.

At the angle of incidence equal to 90° , the lead film did not become separated from graphene after 125 impacts of Xe_{13} clusters. The vertical density profiles $\rho(z)$ of the film that were obtained before the bombardment and after the irradiation of the film by the cluster beam at $\theta = 90^\circ$ are shown in Fig. 4. Two intense peaks of the $\rho(z)$ function for the film that was not subjected to bombardment indicate the presence of two Pb layers that cover the graphene. After bombardment, the loosening and lifting of the film above the graphene occurred; the profile became stretched to $h \approx 0.8$ nm. However, the film did not lose contact with graphene, which is proved by the peak of weak intensity that remained in the vicinity of $h \approx 0.21$ nm.

The change in the stresses in the lead film in the case of vertical impacts ($\theta = 0^\circ$) of Xe_{13} clusters is demonstrated in Fig. 5. It can be seen that the stresses in the film plane increase nonmonotonically during the bombardment and achieve the maximum positive values in the case of σ_{zx} and σ_{zy} and the highest negative values for σ_{zz} in the case of the last (fifth) series of impacts. The stresses that arise during the third series of impacts are minimum, since by the beginning of this period, a cohered stable structure has already formed without strong local stresses. During this series of impacts, stresses start to form in the structure characterized by VPa with $\bar{n} = 13.01$ and $\bar{m} = 4.89$ and, in the case of simplified VPa, the structure with $\bar{n} = 8.37$ and $\bar{m} = 4.58$.

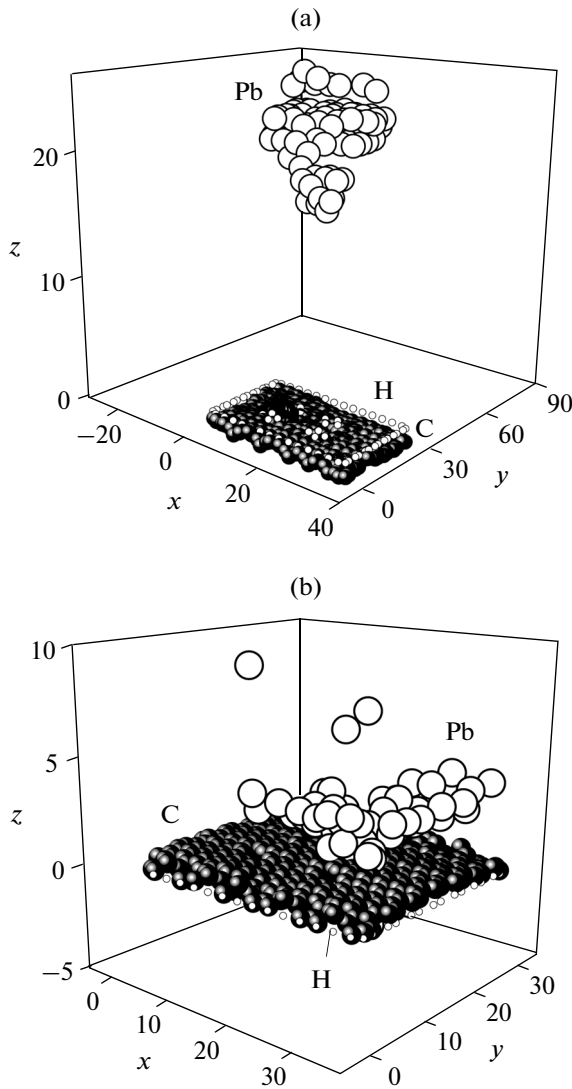


Fig. 3. Configuration of a system of a lead film on a partially hydrogenated imperfect graphene after bombardment with Xe_{13} clusters with an energy equal to 20 eV at the angles of incidence (a) 45° and (b) 75° . The coordinates of atoms are given in angstroms.

The distribution of stresses σ_{zx} , σ_{zy} , and σ_{zz} in graphene both in the zigzag and armchair directions is represented by an alternating-sign aperiodic dependence. As a rule, the amplitudes of stresses in the 5th series of the bombardment are not greater than the amplitude of oscillation of stresses obtained in the first series. This means that they are not strengthened in the course of bombardment. Although most of the time, in the course of bombardment, the graphene sheet was protected from the impacts of Xe_{13} clusters by the metal film, the stresses σ_{zz} in the graphene are significantly higher than the other two types of stresses (σ_{zx} and σ_{zy}). This means that the effect of cluster impacts is transferred to graphene through the lead film.

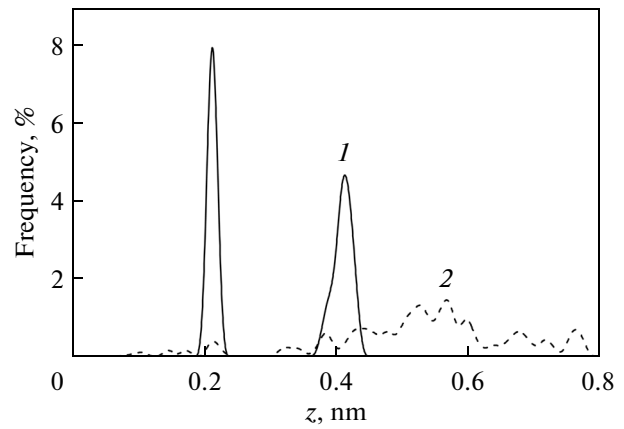


Fig. 4. Vertical profiles of the density of a lead film along the oz axis perpendicular to the graphene plane: (1) before the bombardment; and (2) after the bombardment by clusters with the energy of 20 eV at the angle of incidence equal to 90° . Origin of coordinates coincides with the position of the nearest left-corner apex of the graphene sheet.

The change in the roughness R_a of graphene upon the bombardment at different angles of incidence of Xe_{13} clusters is shown in Fig. 7. It can be seen that, in the second part of the bombardment processes, at angles of cluster incidence of 45° and 60° , the magnitude of R_a is significantly higher than in the case of vertical cluster impacts, i.e., at an incidence angle of 0° . The increase in the angle of incidence to 75° leads to a strong decrease in the magnitude of R_a . In this case, at the end of bombardment, the Pb film is not removed from graphene, and the impacts of Xe_{13} clusters at angles close to glancing are easily reflected by the surface of the target. Here, the magnitude of R_a stays almost unchanged in the course of bombardment.

DISCUSSION

It is of interest to compare the results of the present investigation with the results of [13], where the MD method was used to study the purification of graphene from a copper film by the bombardment with Ar_{13} clusters at a beam energy of 20 eV. The copper film on graphene in [13] was constructed by the method similar to that employed in this work. The difference between the two works is in the film material and in the nature of the inert gas, whose clusters were used as projectiles. Lead atoms are heavier than copper atoms by a factor of 3.26. In correspondence with the difference in the atomic weights of Pb and Cu, a heavier inert gas, xenon ($M_{\text{Xe}}/M_{\text{Ar}} = 3.28$) was chosen for the bombardment of the lead film on the graphene substrate. The complete purification of graphene from copper atoms was achieved only at the angle of incidence equal to 45° . The vertical irradiation ($\theta = 0^\circ$) by Ar_{13} clusters was among most ineffective. In addition,

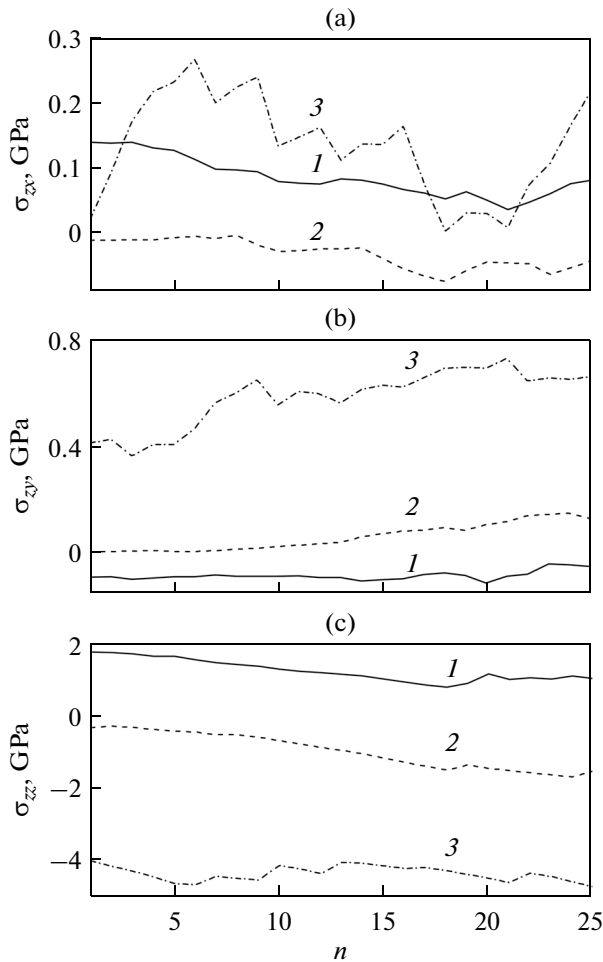


Fig. 5. Main stresses ((a) σ_{xz} , (b) σ_{zy} , and (c) σ_{zz}) in the Pb film vs. the number n of Xe_{13} cluster impacts at the angle of incidence $\theta = 0^\circ$ for (1) series 1, (2) series 3, and (3) series 5 of impacts.

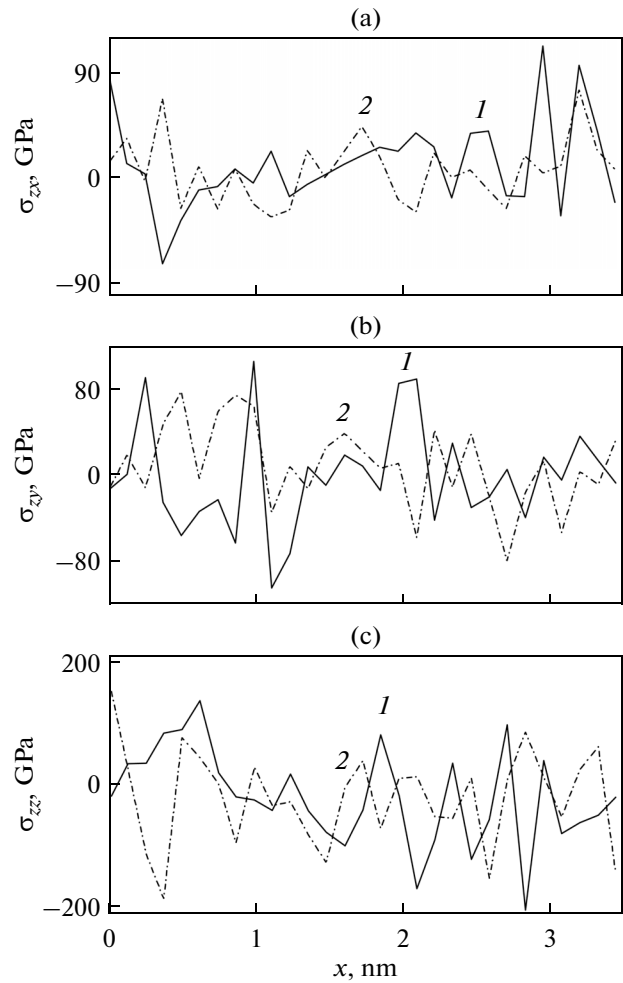


Fig. 6. Distributions of main stresses ((a) σ_{xz} , (b) σ_{zy} , and (c) σ_{zz}) along the zigzag direction in graphene at the angle of incidence of Xe_{13} clusters $\theta = 60^\circ$ after (1) the series 1 of cluster impacts and (2) after the series 5.

in this case, at low beam energies (5 eV), the densification of the Cu film [12] occurred instead of purification. However, the effect of purification of graphene from copper was achieved also at the angle of incidence equal to 90° , i.e., at a glancing angle, at the beam energies of 20 and 30 eV. The removal of copper from graphene occurred mainly via the sequential knocking out of separate atoms. The only common result of computer experiments on the removal of these heavy metals (Cu and Pb) from graphene is the complete purification of the graphene sheet after the bombardment at an angle of incidence equal to 45° . The differences proved to be much stronger. First, in the case of graphene purification from lead, the bombardment at angles of both $\theta = 0^\circ$ and $\theta = 60^\circ$ proved to be efficient; i.e., both resulted in the complete separation of the film from graphene at the beam energy already as low as 10 eV. However, at these angles of incidence and a beam energy of 20 eV, the Pb film is not separated from graphene, since there arise condi-

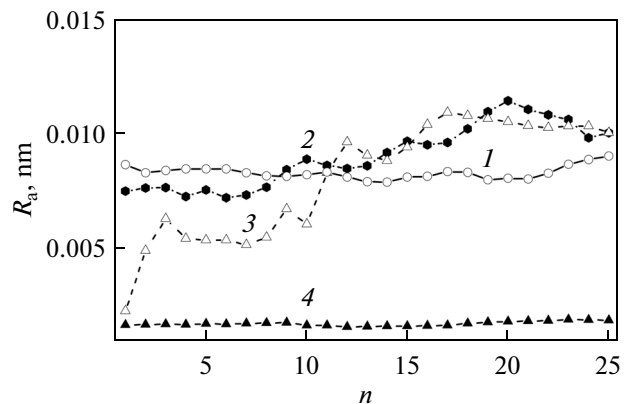


Fig. 7. Roughness of graphene vs. the number of impacts of Xe_{13} clusters for the 5th series at different angles of incidence: (1) 0° , (2) 45° , (3) 60° , and (4) 75° .

tions for nonelastic impacts of atoms in the film, which lead to plastic deformation. Second, at an angle of incidence of 90° , the purification of graphene from Pb atoms was not successful, even at the beam energies of 20 and 30 eV. These differences from the results of computer experiments on the removal of the copper film are explained by a substantially different mechanism of graphene purification from the Pb film. The analysis of the configurations obtained clearly indicates that the prevailing mechanism of separation of the Pb film from graphene is of a predominantly collective character. The connection of graphene with Pb atoms is weaker than with Cu atoms. At the same time, the interaction between Pb atoms is long-range and rather strong. Only very precise impacts of Xe atoms knock out separate Pb atoms from the film. Under cluster impacts, a rather large island of the film gradually is separated from graphene. This occurs due to impacts of the reflected Xe atoms, as well as of the knocked-out Pb atoms. A significant flat part of the film separated from graphene to several interatomic distances does not interact further with graphene and starts taking a spherical shape, i.e., the shape of a cluster having the minimum surface area. The impacts of Xe atoms on the island also favor the faster transition from a two- to three-dimensional system. Because of the island mechanism of the separation of the Pb film from graphene, the purification of the graphene sheet at an angle of cluster incidence equal to 90° proves to be unsuccessful. On one hand, the mechanism of separation of the island from graphene does not work in this case, since no reflected Xe atoms that lift the island vertically exist here. On the other hand, even Xe_{13} clusters with the energy of 30 eV are not able to move a heavy island connected to C atoms along the graphene plane. The presence of H atoms on graphene only plays an insignificant role in the separation of lead from graphene. Therefore, the hydrogenation of the graphene edges appeared to be effective at protecting graphene edges from damages caused by impacts of the high-velocity Xe atoms.

CONCLUSIONS

A series of molecular-dynamic calculations that simulate the bombardment of a thin lead film on modified graphene at different angles of incidence of a beam of Xe_{13} clusters with an energy of 20 eV has been performed. The investigation of the structure of the deposited metal film on graphene by the method of statistical geometry has demonstrated an irregular character of distribution of Pb atoms in the central part of the film with a prevailing rotational symmetry of the fifth order. In the case of an inclined irradiation of the target by the Xe_{13} clusters with an energy of 20 eV, the complete purification of graphene from lead was accomplished at an angle of incidence equal to 45° . The process of the separation of lead from

graphene has a mainly collective character due to the weak connection of metal atoms with the substrate and a comparatively stronger long-range interaction between the atoms in the film. In the course of the vertical incidence of the cluster beam, the first two series of the cluster impacts densify the film, leading to a more regular packing of atoms in it and to a relief of the internal stresses. The further series of impacts promote an increase in internal stresses. The stresses in graphene only weakly depend on the angle of incidence of the cluster beam and are not strengthened in the course of bombardment. The final magnitudes of the roughness of graphene caused by the cluster bombardment vary within 10% with the change in the angle of incidence from 0° to 60° . The roughness decreases substantially at the angle of incidence of 75° . The graphene with hydrogenated edges and boundaries of divacancies does not suffer significant damages at all investigated angles of incidence at the cluster energy of 20 eV. The inclined ($\theta = 45^\circ$) bombardment by xenon clusters with the kinetic energies of 20 eV can be employed to clean graphene membranes of adsorbed lead.

ACKNOWLEDGMENTS

This work was performed within the framework of a state task of the FANO of the Russian Federation (theme "Electrode Reactions of Electrochemical Technologies of Refining and Obtaining Metals and Their Compounds in Molten Salts," no. 0395-2014-0004) and was supported in part by the Russian Foundation for Basic Research (project no. 13-08-00273).

REFERENCES

1. S. N. Luoma, "Bioavailability of trace metals to aquatic organisms. A review," *Sci. Total Environ.* **28**, 1–22 (1983).
2. W. Hummers and R. Offeman, "Preparation of graphitic oxide," *J. Am. Chem. Soc.* **80**, 1339–1339 (1958).
3. L. Zaijan, Y. Yuling, T. Jian, and P. Jiaomai, "Spectrophotometric determination of trace lead in water after preconcentration using mercaptosephadex," *Talanta* **60**, 123–130 (2003).
4. M. S. Di Nezio, M. E. Palomeque, and B. S. Fernandez, "A sensitive spectrophotometric method for lead determination by flow injection analysis with on-line preconcentration," *Talanta* **63**, 405–409 (2004).
5. D. Kara, M. Alkan, and U. Cakir, "Solvent extraction of copper from aqueous solution with pentaeritryl tetra-rabenzylamine," *Turk. J. Chem.* **25**, 293–303 (2001).
6. S. B. Sonawale, Y. V. Ghalsasi, and A. P. Argekar, "Extraction of lead(II) and copper(II) from salicylate media by tributylphosphine oxide," *Anal. Sci.* **17**, 285–289 (2001).
7. J. L. Manzoori and A. T. Bavili, "Cloud point preconcentration and flame atomic absorption spectrometric

- determination of Cd and Pb in human hair,” *Anal. Chim. Acta* **470**, 215–221 (2002).
8. J. Chen and K. C. Teo, “Determination of cadmium, copper, lead and zinc in water samples by flame atomic absorption spectrometry after cloud point extraction,” *Anal. Chim. Acta* **450**, 215–222 (2001).
 9. S. Yuan, W. Chen, and S. Hu, “Simultaneous determination of cadmium (II) and lead (II) with clay nanoparticles and anthraquinone complexly modified glassy carbon electrode,” *Talanta* **64**, 922–928 (2004).
 10. H. Gao, J. Zhou, M. Lu, W. Fa, and Y. Chen, “First-principles study of the IVA group atoms adsorption on graphene,” *J. Appl. Phys.* **107**, 114311 (2010).
 11. D. Ma and Z. Yang, “First-principles studies of Pb doping in graphene: Stability, energy gap and spin-orbit splitting,” *New J. Phys.* **13**, 123018 (2011).
 12. A. E. Galashev and V. A. Polukhin, “Compaction of a copper film on graphene by argon-beam bombardment: Computer experiment,” *J. Surf. Invest. X-ray, Synchr. Neutr. Tech.* **8**, 1082–1088 (2014).
 13. A. E. Galashev and V. A. Polukhin, “Removal of copper from graphene by bombardment with argon clusters: Computer experiment,” *Phys. Met. Metallogr.* **115**, 697–704 (2014).
 14. A. E. Galashev and O. R. Rakhmanova, “Mechanical and thermal stability of graphene and graphene-based materials,” *Phys.-Usp.* **57**, 970–989 (2014).
 15. A. E. Galashev and A. A. Galasheva, “Molecular dynamics simulation of copper removal from graphene by bombardment with argon clusters,” *High Energy Chem.* **48**, 112–116 (2014).
 16. M. F. Jr. Russo and B. J. Garrison, “Mesoscale energy deposition footprint model for kiloelectronvolt cluster bombardment of solids,” *Anal. Chem.* **78**, 7206–7210 (2006).
 17. M. F. Jr. Russo, C. Szakal, J. Kozole, N. Winograd, and B. J. Garrison, “Sputtering yields for C₆₀ and Au₃ bombardment of water ice as a function of incident kinetic energy,” *Anal. Chem.* **79**, 4493–4498 (2007).
 18. E. J. Smiley, N. Winograd, and B. J. Garrison, “Effect of cluster size in kiloelectronvolt cluster bombardment of solid benzene,” *Anal. Chem.* **79**, 494–499 (2007).
 19. Y. Watanabe, H. Yamaguchi, M. Hashinokuchi, K. Sawabe, S. Maruyama, Y. Matsumoto, and K. Shobatake, “Trampoline motions in Xe-graphite (0001) surface scattering,” *Chem. Phys. Lett.* **413**, 331–334 (2005).
 20. J. Tersoff, “Empirical interatomic potential for carbon, with application to amorphous carbon,” *Phys. Rev. Lett.* **61**, 2879–2882 (1988).
 21. S. J. Stuart, A. V. Tutein, and J. A. Harrison, “A reactive potential for hydrocarbons with intermolecular interactions,” *J. Chem. Phys.* **112**, 6472–6486 (2000).
 22. A. E. Galashev and V. A. Polukhin, “Computer study of the physical properties of a copper film on a heated graphene surface,” *Phys. Solid State* **55**, 1733–1738 (2013).
 23. A. E. Galashev and S. Yu. Dubovik, “Molecular dynamics simulation of compression of single-layer graphene,” *Phys. Solid State* **55**, 1976–1983 (2013).
 24. H. Rafii-Tabar, “Modelling the nano-scale phenomena in condensed matter physics via computer-based numerical simulations,” *Phys. Rep.* **325**, 239–310 (2000).
 25. Y. M. Kim and S.-C. Kim, “Adsorption/desorption isotherm of nitrogen in carbon micropores,” *J. Korean Phys. Soc.* **40**, 293–299 (2002).
 26. A. Arkundato, Z. Su’ud, M. Abdullah, and W. Sutrisno, “Study of liquid lead corrosion of fast nuclear reactor and its mitigation by using molecular dynamics method,” *Int. J. Appl. Phys. Math.* **3**, 1–7 (2013).
 27. F.-Y. Li and R. S. Berry, “Dynamics of Xe atoms in NaA zeolites and the 129Xe chemical shift,” *J. Phys. Chem.* **99**, 2459–2468 (1995).
 28. J. F. Ziegler, J. P. Biersack, and U. Littmark, *Stopping and Ranges of Ions in Matter* (Pergamon, New York, 1985), Vol. 1.
 29. A. Delcorte and B. J. Garrison, “High yield events of molecule emission induced by keV particle bombardment,” *J. Phys. Chem. B* **104**, 6785–6800 (2000).
 30. F. D. Lamari and D. Levesque, “Hydrogen adsorption on functionalized graphene,” *Carbon* **49**, 5196–5200 (2011).
 31. H. J. C. Berendsen, J. P. M. Postma, W. F. van Gunsteren, A. DiNola, and J. R. Haak, “Molecular dynamics with coupling to an external bath,” *J. Chem. Phys.* **81**, 3684–3690 (1984).
 32. B. Hafskjold and T. Ikeshoji, “Microscopic pressure tensor for hard-sphere fluids,” *Phys. Rev. E: Stat., Nonlin., Soft Matter Phys.*, **66**, 011203 (2002).
 33. S. Yu. Davydov, “Energy of substitution of atoms in the epitaxial graphene–buffer layer–SiC substrate system,” *Phys. Solid State* **54**, 875–882 (2012).
 34. Z. H. Jin, H. W. Sheng, and K. Lu, “Melting of Pb clusters without free surfaces,” *Phys. Rev. B: Condens. Matter Mater. Phys.* **60**, 141–149 (1999).

Translated by S. Gorin